the number of seeds and the result is that the final crystallites will be small. In many industrial processes, the control of crystallite size is important. The present work suggests that a careful selection of the size of the crystallization promoter can be of crucial importance.

Real-space imaging techniques, such as the ones used to study crystallization in colloidal suspensions[12], could be used to study seeded crystal nucleation in real colloidal systems. In such experiments, relatively large colloidal beads (spheres) or glass fibres (cylinders) could be introduced in a supersaturated solution of monodisperse, 'hard sphere' colloids. Crystallization should take place readily on the larger seeds. Owing to gravity, crystal nuclei that detach from the seed should sediment away from it. This should make it easier to image subsequent crystal nucleation events on the same seed. □

Received 9 September 2003; accepted 3 February 2004; doi:10.1038/nature02397.

1. Ostwald, W. F. Studien uber die Bildung und Umwandlung fester Korper. *Z. Phys. Chem.* **22,** 289–302 (1897).
2. Kelton, K. E. in *Solid State Physics* (eds Ehrenreich, H. & Turnbull, D.) Vol. 45 (Academic, New York, 1991).
3. ten Wolde, P. R., Ruiz-Montero, M. J. & Frenkel, D. Numerical calculation of the rate of crystal nucleation in a Lennard-Jones system at moderate undercooling. *J. Chem. Phys.* **104,** 9932–9947 (1996).
4. Auer, S. & Frenkel, D. Quantitative prediction of crystal nucleation rates for spherical colloids: A computational approach. *Annu. Rev. Phys. Chem.* **55,** (2004).
5. Kose, A. & Hachisu, S. Ordered structure in weakly flocculated monodisperse latex. *J. Colloid Interf. Sci.* **55,** 487–498 (1976).
6. Dinsmore, A., Warren, P., Poon, W. & Yodh, A. Fluid-solid transitions on walls in binary hard-sphere mixtures. *Europhys. Lett.* **40,** 337–342 (1997).
7. Kaplan, P., Rouke, J., Yodh, A. & Pine, D. Entropically driven surface phase separation in binary colloidal mixtures. *Phys. Rev. Lett.* **72,** 582–585 (1994).
8. Auer, S. & Frenkel, D. Line tension controls wall-induced crystal nucleation in hard-sphere colloids. *Phys. Rev. Lett.* **91,** 015703 (2003).
9. Euler, L. *Opera Omnia* Series i, Vol. 26 (Orell Füssli, Zurich, 1953).
10. Hilton, P. & Pederson, J. The Euler characteristic and Pólya's dream. *Am. Math. Mon.* **103,** 121–131 (1996).
11. Auer, S. & Frenkel, D. Suppression of crystal nucleation in polydisperse colloids due to increase of the surface free energy. *Nature* **413,** 711–713 (2001).
12. Gasser, U., Weeks, E. R., Schofield, A., Pussey, P. N. & Weitz, D. A. Real-space imaging of nucleation and growth in colloidal crystallization. *Science* **292,** 258–262 (2001).

Acknowledgements The work of the FOM Institute is part of the research program of FOM and is made possible by financial support from the Netherlands Organization for Scientific Research (NWO).

Competing interests statement The authors declare that they have no competing financial interests.

Correspondence and requests for materials should be addressed to A.C. (cacciuto@amolf.nl).

Mass and volume contributions to twentieth-century global sea level rise

Laury Miller[1] **& Bruce C. Douglas**[2]

[1]*Laboratory for Satellite Altimetry, NESDIS, NOAA, Silver Spring, Maryland 20910, USA*
[2]*Laboratory for Coastal Research, Florida International University, Miami, Florida 33199, USA*

The rate of twentieth-century global sea level rise and its causes are the subjects of intense controversy[1–7]. Most direct estimates from tide gauges give 1.5–2.0 mm yr^{-1}, whereas indirect estimates based on the two processes responsible for global sea level rise, namely mass and volume change, fall far below this range. Estimates of the volume increase due to ocean warming give a rate of about 0.5 mm yr^{-1} (ref. 8) and the rate due to mass increase, primarily from the melting of continental ice, is thought to be even smaller. Therefore, either the tide gauge estimates are too high, as has been suggested recently[6], or one (or both) of the mass and volume estimates is too low. Here we present an analysis of sea level measurements at tide gauges combined with observations of temperature and salinity in the Pacific and Atlantic oceans close to the gauges. We find that gauge-determined rates of sea level rise, which encompass both mass and volume changes, are two to three times higher than the rates due to volume change derived from temperature and salinity data. Our analysis supports earlier studies that put the twentieth-century rate in the 1.5–2.0 mm yr^{-1} range, but more importantly it suggests that mass increase plays a larger role than ocean warming in twentieth-century global sea level rise.

At the time of the second IPCC assessment in 1995[9], there seemed to be little controversy regarding global sea level rise (GSLR). Most gauge estimates fell in the range 1.5–2.0 mm yr^{-1}. Most of this rise was thought to result from ocean warming, with the rest due to melting of continental ice. However, by the third IPCC assessment in 2001[1], this consensus view had collapsed: new and better estimates of ocean warming had reduced the volume increase component to about 0.5 mm yr^{-1} (ref. 8), and the mass component was thought to be even smaller. This left a large unexplained gap between direct and indirect estimates of GSLR, now known as the 'attribution problem'.

Two recent studies offer opposing solutions to this dilemma. Cabanes *et al.*[6] argue that gauge rates are 2–3 times too high because the gauges happen to be located in areas of abnormally high ocean warming. They arrive at this result by comparing gauge-derived sea level trends with those obtained from objectively interpolated hydrographic measurements, concluding that the true rate of GSLR is actually 0.5–1.0 mm yr^{-1}, mostly due to ocean warming. This solution provides a way out of the attribution problem, but implies a huge acceleration of GSLR in the 1990s if recent satellite altimetric estimates of ~2.5 mm yr^{-1} (ref. 10) are to be believed. Alternatively, Antonov *et al.*[7] suggest that the problem may be solved by revising upward the mass component estimate. They show that the oceans are freshening at a rate equivalent to the addition of 1.4 mm yr^{-1} of fresh water, approximately the value needed to bring the mass plus volume rate close to the gauge rate. However, this solution assumes a continental ice source rather than floating ice, a key point that they are unable to demonstrate.

Here we present a simple approach to the problem of distinguishing between mass and volume contributions to GSLR. We identify large areas in the Pacific and Atlantic oceans that are either bounded by, or adjacent to, several gauge sites exhibiting similar trends and variability. For those regions, we compare average gauge trends (which reflect both mass and volume change) with average dynamic height trends (which reflect only volume change), with the added distinction that we use raw rather than interpolated hydrographic data. In most areas, the difference between raw and interpolated data are unimportant. However, as shown below, the interpolated data used by Cabanes *et al.*[6] contains errors near the Gulf Stream large enough to cause their average warming estimate for the gauge sites to be biased upward by a factor of 2–3. In contrast, we find no evidence that the gauges are located in regions of abnormally high warming.

We begin in the Eastern Pacific in a region bounded by gauge sites at Honolulu, San Francisco, San Diego, and Balboa, Panama (map inset, Fig. 1). This region has several characteristics that make it ideal for this study: low mesoscale variability, narrow continental margins, large numbers of hydrographic observations, and long (>90 yr) gauge records. Figure 1 presents ~19,000 dynamic height anomaly observations relative to 1,000 m, their 5-yr running means, and 5-yr running means of the four gauge records. Although the hydrographic data appear noisy in this plot, their r.m.s., 6.7 cm, is comparable to satellite altimeter determinations of sea level variability in this relatively quiet part of the global ocean[11]. A linear

regression on the smoothed dynamic heights indicates an upward trend of 0.5 mm yr^{-1} between 1932 and 1997. Similar trends are found when the calculations are performed on the much smaller numbers of observations reaching 2,000 m and 3,000 m (3,174 and 2,119, respectively).

In contrast to the hydrographic results, all four gauge records show trends of ~2 mm yr^{-1} during the twentieth century, despite the fact that the gauge sites are widely separated and thus subject to different vertical land motions and local hydrographic conditions. Additional evidence that the gauges are observing the same regional trend comes from the fact that all four records also show similar interannual variations dominated by El Niño events.

Could the discrepancy between the gauge-derived and hydrographic-measurement-derived trends in Fig. 1 be explained by unusually high rates of warming near the gauge sites? Figure 2 shows sea level and dynamic height comparisons for three local areas encompassing (or adjacent to) the gauge sites. Because of strong similarities between the San Francisco and San Diego gauge records, the California coast is treated as one region in Fig. 2a. California and Honolulu (Fig. 2a, b) yield 1,000-m dynamic height trends of 0.5 mm yr^{-1} and 0.3 mm yr^{-1} from 1938 to 1996 and 1950 to 1999, respectively. Extending the hydrographic analysis in either of these locations to 2,000 m does not significantly change the results (there are insufficient hydrographic data in either region to go to 3,000 m). Balboa (Fig. 2c) exhibits a larger 1,000-m dynamic height trend, 0.9 mm yr^{-1}, but still only half the matching gauge trend of 1.7 mm yr^{-1} over the interval 1930–1993. Results from each local area in the eastern Pacific therefore support the conclusion summarized in Fig. 1: that twentieth-century sea level rose at a rate several times higher than can be accounted for by volume (temperature and salinity) changes alone.

Figure 3 shows a comparison of dynamic height and sea level trends in the eastern North Atlantic, another area with low mesoscale variability, narrow margins, and so on. The dynamic height trend there is only 0.2 mm yr^{-1} from 1911 to 1998. In contrast, the gauges at Cascais (Portugal) and Tenerife (Canary Islands) show sea level trends of 2.1 and 1.9 mm yr^{-1}, respectively, an order of magnitude greater than the hydrographic data. Extending the hydrographic analysis more deeply into the water column does not significantly alter this result.

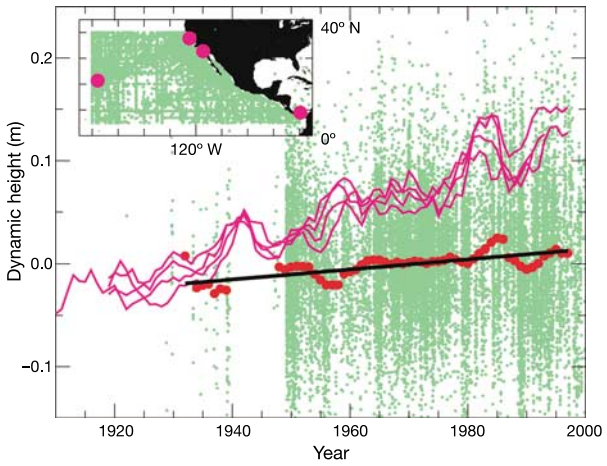

Figure 1 Regional comparison of hydrographic and tide-gauge-measured sea level change in the Eastern Pacific. Hydrographic profile observations of temperature and salinity converted into 1,000-m dynamic height anomalies (green), their 5-yr running means (red data points) and linear regression (black) compared with 5-yr running mean relative sea levels from tide gauge observations at San Francisco, San Diego, Honolulu and Balboa (purple lines). Tide gauge series have been vertically offset to coincide with the earliest dynamic heights. Map inset shows tide gauge locations in purple and observed dynamic height locations in green.

Finally, Fig. 4 presents an analysis of the Slope Water region in the western North Atlantic, north of the Gulf Stream and east of the tide gauge sites at Boston, Portland and Halifax. Two types of dynamic height data are shown. The green dots, and their 5-yr means in red, represent dynamic height anomalies computed from observed temperature and salinity measurements, as in Figs 1–3. The blue curves represent anomaly values computed from the World Ocean Atlas 1998v2 (WOA98v2)[12], the objectively interpolated hydrographic data set used by Cabanes *et al.*[6].

As in the eastern Pacific and Atlantic, the gauge records exhibit substantially higher trends, an average 1.9 mm yr^{-1} during the twentieth century, than those based on the observed hydrographic data. In fact, the trends on the latter are negligible over the record (1931–1996). By contrast, the results based on the WOA98v2 analysis exhibit an abrupt 20-cm increase between 1965 and 1975 that is not present in either the surrounding hydrographic observations or gauge records. Over the 1955–1996 interval used by Cabanes *et al.*[6], the average WOA98v2-derived trend is 6.7 mm yr^{-1}, more than three times greater than the corresponding gauge trend.

There is good reason to believe that this 'jump' is an artefact of the large (444 to 888 km) variable radius of influence used in the

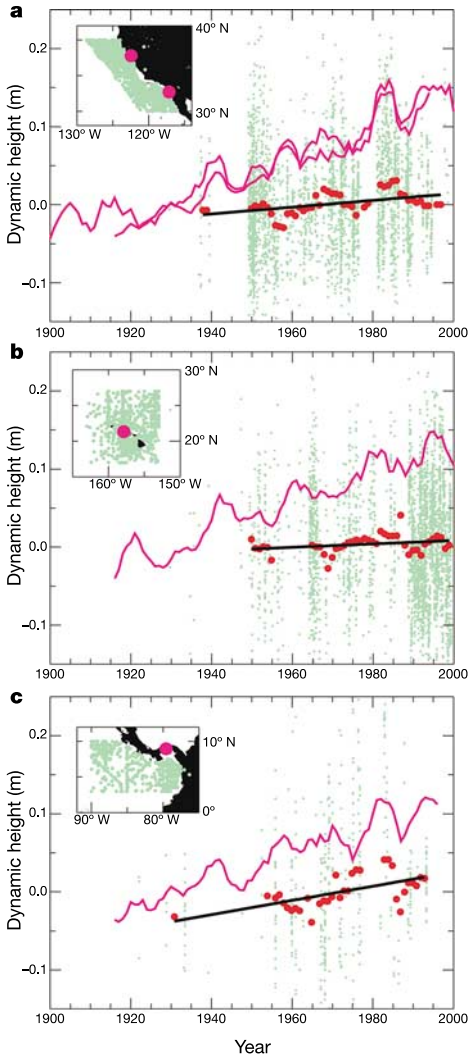

Figure 2 Local comparison of hydrographic and tide-gauge-measured sea level change. **a**, As in Fig. 1, but hydrographic observations limited to 4,400 km × 1,100 km area adjacent to gauge sites at San Francisco and San Diego; **b**, to 1,100 km × 1,100 km area centred on gauge site at Honolulu; **c**, to 800 km × 1,400 km area adjacent to gauge site at Balboa, Panama.

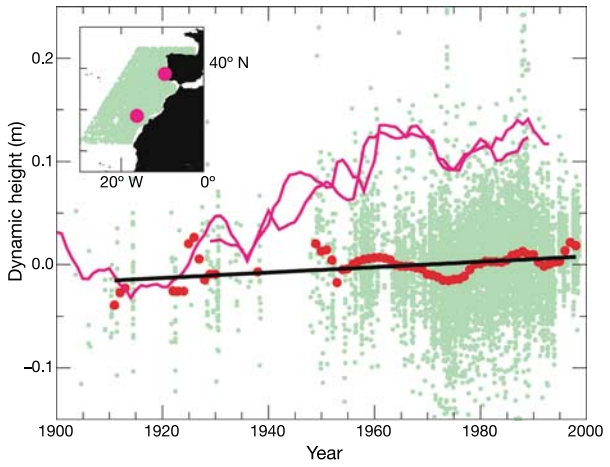

Figure 3 Regional comparison of hydrographic and tide-gauge-measured sea level change in the Eastern Atlantic. As in Fig. 1, but hydrographic observations limited to 1,400 km × 2,200 km area adjacent to tide gauge sites at Cascais (Portugal) and Tenerife (Canary Islands).

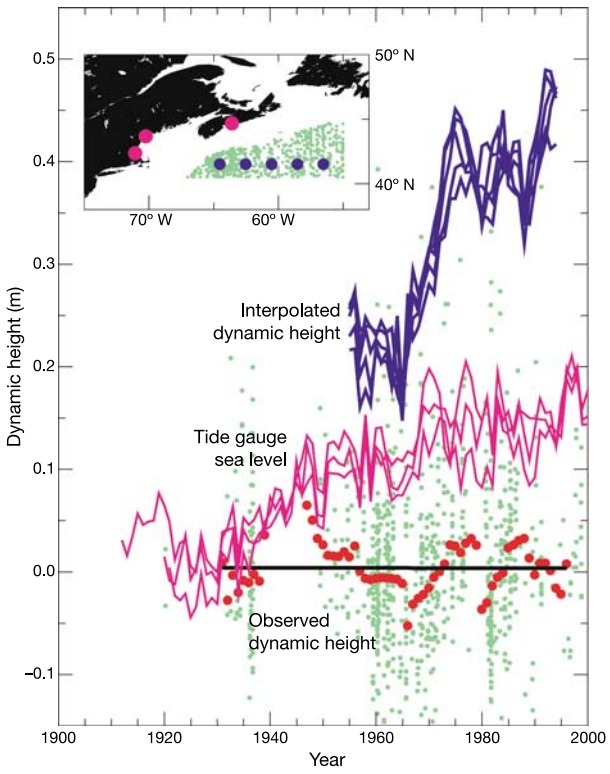

Figure 4 Regional comparison of hydrographic and tide-gauge-measured sea level change in the Western Atlantic. As in Fig. 1, but hydrographic observations limited to 1.300 km × 500 km triangular region adjacent to tide gauge sites at Boston, Portland and Halifax. Time series of dynamic height anomalies computed from the WOA98v2 interpolated data set are shown in blue, offset by 0.4 m. Map inset shows tide gauge locations in purple, observed dynamic height locations in green and interpolated dynamic height locations in blue.

WOA98v2 objective analysis. Between the mid-1960s and early 1970s, the mean position of the Gulf Stream shifted northward by about 50 km as a result of gyre-scale changes in the surface wind field[13]. An examination of the actual hydrographic observations taken during this period shows a dynamic height rise of about 20 cm confined to a zonal band about 100 km wide, that is, the width of the Gulf Stream, and negligible change to the north or south. However, the WOA98v2 analysis shows this 20-cm signal covering a much wider area, including all of the Slope Water region shoreward of the Gulf Stream, between Cape Hatteras and Newfoundland. In contrast, none of the gauges along the east coast of North America show a 20-cm rise in the 1970s. To assess the impact of this error on the calculation by Cabanes *et al.*[6] of the average warming-induced rise for their nine study areas, assuming a minimal rate of 0.5 mm yr^{-1} for eight of their regions and 6.7 mm yr^{-1} for the northeast coast of North America, yields an average rate of 1.2 mm yr^{-1}, which is 2–3 times greater than global estimates of the warming effect[8]. Thus nearly all of the alleged anomalous local effects in the study by Cabanes *et al.*[6] can be explained by errors in the WOA98v2 analysis.

Our results help to resolve two aspects of the present controversy over twentieth-century GSLR. Concerning the question of whether or not the gauge results are biased high owing to above-average local ocean warming, we conclude that they are not. It follows that the weight of direct evidence strongly suggests a rate of 1.5–2.0 mm yr^{-1} for twentieth-century GSLR. This is in agreement with most traditional estimates from long gauge records, and is reasonably consistent with the ~2.5 mm yr^{-1} rate obtained by ongoing satellite altimeters for the period 1993–2003.

Concerning the causes of sea level rise, our results provide clear evidence that changes in ocean volume due to temperature and salinity account for only a fraction of sea level change, and that mass change plays a dominant role in twentieth-century GSLR. This aspect of our results is consistent with the results of Antonov *et al.*[7], who show that the global oceans freshened during the latter half of the twentieth century by an amount equivalent to 1.4 mm yr^{-1} of fresh water, but goes further by indicating that the source must be continental. The only alternative to this interpretation is that what we identify as mass change is actually a mass redistribution within the global ocean rather than a mass increase due to the addition of fresh water. However, for this to be true, large areas of the global ocean would have to have falling sea levels for the entire twentieth century. Observations from the global tide gauge network, consisting mostly of gauge sites located along the margins of the ocean basins, do not support this viewpoint. Whether the mid-oceans are currently undergoing such changes can only be determined from long-term, high-precision satellite altimeter missions, such as the TOPEX/Poseidon and Jason missions, which are at present under way. □

Methods

Data sources

All of the tide gauge records used in this study were obtained from the Permanent Service for Mean Sea Level (PSMSL)[14] in the form of monthly average relative sea level measurements. Each record was corrected for vertical land motion due to glacial isostatic adjustment[15], but not for the inverted barometer effect caused by atmospheric pressure variations. The PSMSL[14] in its table of trends shows formal errors (SD) of about 0.2–0.4 mm yr^{-1} for records >60 yr. The uncertainty of our trends derived from independent 5-yr gauge means is 0.1–0.3 mm yr^{-1}, less because of the further smoothing beyond 1 yr.

Observed (as opposed to interpolated) hydrographic profile data were obtained from the World Ocean Atlas 1998v2[12] and density (steric) changes computed from both temperature and salinity variability. To avoid over-weighting the data set with shallow expendable bathythermograph (XBT) measurements, only traditional bottle, salinity–temperature–depth (STD), and conductivity–temperature–depth (CTD) measurements to 500 m or more were used. Surface dynamic heights (0 to 500 m, to 1,000 m, and so on) were calculated for each profile by computing specific volume anomalies at observed levels and then integrating in the vertical. In order to correctly average over regions with significant variation of mean dynamic topography, dynamic height deviations were computed relative to a 1° × 1° (or in data-sparse areas, 2° × 2°) mean dynamic topography interpolated to the actual location of each observation. These deviations were subsequently converted into dynamic height anomalies by subtracting mean annual and semi-annual cycles based on a least-squares fit to the month-by-month composite of all measurements within a given region.

Weighting and sampling

Because hydrographic observations tend to be concentrated near land or along specific track lines and there is evidence of geographical variations in the steric trends, it is important to consider how area weighting might lead to a different estimate of the trend for a particular region. To this end, we computed 1,000-m dynamic height trends for each 10° × 10° area in the eastern Pacific study area shown in Fig. 1. The results range between 0.1

and 1.8 mm yr^{-1} with a regional average value of 0.8 mm yr^{-1}. Although this figure is somewhat higher than the trend computed without area weighting, the difference is not significant considering the poor temporal sampling found in several of the 10° × 10° areas. Thus, we conclude that area weighting is not essential to this study. The formal uncertainties of trends of dynamic height derived from 5-yr means are 0.1–0.2 mm yr^{-1}. These are smaller than the uncertainty values from gauge data because the former are based on area averages.

Except for the Balboa area, which suffers from relatively poor temporal sampling, the hydrographic results presented in Fig. 2 are not overly sensitive to the size or orientation of the sample areas. Cutting the width of the California area in half, that is, setting the offshore boundary at 220 km instead of 440 km as shown, results in a dynamic height trend of 0.4 mm yr^{-1} instead of 0.5 mm yr^{-1} over 1938–1996. Similarly, cutting the Honolulu area in half results in a dynamic height trend of 0.4 mm yr^{-1} instead of 0.3 mm yr^{-1} from 1950 to 1999.

Received 15 July; accepted 22 December 2003; doi:10.1038/nature02309.

1. Church, J. A. *et al. Climate Change 2001: The Scientific Basis* (ed. Houghton, J. T.) Ch. 11 (Cambridge Univ. Press, New York, 2001).
2. Douglas, B. C. & Peltier, W. R. The puzzle of global sea level rise. *Phys. Today* **55**(3), 35–40 (2002).
3. Munk, W. Twentieth century sea level: an enigma. *Proc. Natl Acad. Sci. USA* **99,** 6550–6555 (2002).
4. Meier, M. & Wahr, J. M. Sea level is rising: do we know why? *Proc. Natl Acad. Sci. USA* **99,** 6524–6526 (2002).
5. Munk, W. Ocean freshening, sea level rising. *Science* **300,** 2041–2043 (2003).
6. Cabanes, C., Cazenave, A. & LeProvost, C. Sea level rise during past 40 years determined from satellite and in situ observations. *Science* **294,** 840–842 (2001).
7. Antonov, J. I., Levitus, S. & Boyer, T. P. Steric sea level variations 1957–1994: importance of salinity. *J. Geophys. Res.* **107,** doi:10.1029/200/JC000964 (2002).
8. Levitus, S., Antonov, J. I., Boyer, T. P. & Stephens, C. Warming of the world ocean. *Science* **287,** 2225–2229 (2000).
9. Warrick, R. A., Le Provost, C., Meier, M. F., Oerlemans, J. & Woodworth, P. L. in *Climate Change 1995, The Science of Climate Change* (eds Houghton, J. T. *et al.*) 359–405 (Cambridge Univ. Press, Cambridge, 1996).
10. Nerem, R. S. & Mitchum, G. T. in *Sea Level Rise; History and Consequences* (eds Douglas, B. C., Kearney, M. S. & Leatherman, S. P.) 65–95 (Academic, San Diego, 2001).
11. Ducet, N., Le Traon, P. Y. & Reverdin, G. Global high-resolution mapping of ocean circulation from TOPEX/Poseidon and ERS-1 and -2. *J. Geophys. Res. C* **105,** 19477–19498 (2002).
12. World Ocean Atlas 1998v2. ⟨http://www.nodc.noaa.gov/OC5/wod98v2.html⟩
13. Joyce, T. M., Deser, C. & Spall, M. A. The relation between decadal variability of Subtropical Mode Water and the North Atlantic Oscillation. *J. Clim.* **13,** 2550–2569 (2000).
14. Permanent Service for Mean Sea Level ⟨http://www.pol.ac.uk/psmsl/psmsl_individual_stations.html⟩ (accessed 2003).
15. Peltier, W. R. in *Sea Level Rise; History and Consequences* (eds Douglas, B. C., Kearney, M. S. & Leatherman, S. P.) 65–95 (Academic, San Diego, 2001).

Acknowledgements We thank G. Mitchum for comments and suggestions; T. Rossby, P. Woodworth, S. Gille, R. Cheney, J. Lillibridge, W. Smith and B. Miller for insights; and C. Y. Kuo and C. K. Shum for sharing their computations based on the WOA98 interpolated data set. This work was supported in part by NOAA's Climate Services and Observations Program and NASA. The views, opinions, and findings contained in this report are those of the authors, and should not be construed as an official NOAA or US Government position, policy or decision.

Competing interests statement The authors declare that they have no competing financial interests.

Correspondence and requests for materials should be addressed to L.M. (laury.miller@noaa.gov).

Experimental evidence for the existence of iron-rich metal in the Earth's lower mantle

Daniel J. Frost[1], Christian Liebske[1], Falko Langenhorst[1], Catherine A. McCammon[1], Reidar G. Trønnes[1,2] & David C. Rubie[1]

[1]*Bayerisches Geoinstitut, University of Bayreuth, D-95440 Bayreuth, Germany*
[2]*Nordic Volcanological Institute, Natural Sciences Building, University of Iceland, IS-101, Reykjavík, Iceland*

The oxidation state recorded by rocks from the Earth's upper mantle can be calculated from measurements of the distribution of Fe^{3+} and Fe^{2+} between the constituent minerals[1–3]. The capacity for minerals to incorporate Fe^{3+} may also be a significant factor controlling the oxidation state of the mantle[4,5], and high-pressure experimental measurements of this property might provide important insights into the redox state of the more inaccessible deeper mantle. Here we show experimentally that the Fe^{3+} content of aluminous silicate perovskite, the dominant lower-mantle mineral, is independent of oxygen fugacity. High levels of Fe^{3+} are present in perovskite even when it is in chemical equilibrium with metallic iron. Silicate perovskite in the lower mantle will, therefore, have an Fe^{3+}/total Fe ratio of at least 0.6, resulting in a whole-rock ratio of over ten times that of the upper mantle[5,6]. Consequently, the lower mantle must either be enriched in Fe^{3+} or Fe^{3+} must form by the disproportionation of Fe^{2+} to produce Fe^{3+} plus iron metal. We argue that the lower mantle contains approximately 1 wt% of a metallic iron-rich alloy. The mantle's oxidation state and siderophile element budget have probably been influenced by the presence of this alloy.

The Earth's upper mantle contains both ferric and ferrous iron but ferrous iron is by far the more dominant species ($Fe^{3+}/\Sigma Fe < 0.03$) (refs 5, 6). Chemical equilibria between Fe^{3+}- and Fe^{2+}-bearing minerals in mantle rocks can be used to calculate the oxygen fugacity of the upper mantle, which is generally found to fall within +1 and −2 log units of the quartz–fayalite–magnetite oxygen buffer[1–3]. This lower bound is more than three orders of magnitude above the level where the upper mantle would be in chemical equilibrium with metallic iron, as probably occurred during core–mantle segregation.

The oxygen fugacity of an upper-mantle assemblage equates quite reasonably with the concentration of Fe^{3+} in some constituent minerals. The Fe^{3+} content of spinel, for example, decreases with decreasing oxygen fugacity towards zero at conditions of equilibrium with metallic iron[3]. This relationship is dependent on mineral structure and chemistry, however, and at higher pressures there are examples of silicate minerals (such as wadsleyite, ringwoodite and majoritic garnet) that have significant Fe^{3+} concentrations when coexisting with metallic iron[4,5]. The crystal–chemical constraints that make Fe^{2+} the dominant iron species in the upper mantle may not, therefore, hold for the transition zone and lower mantle, where mixtures of Fe^{3+}-rich minerals and metallic Fe may become stable, even if bulk oxygen contents are the same as in the upper mantle.

Using a multianvil high-pressure apparatus, we have synthesized samples of aluminous silicate perovskite coexisting with metallic Fe to determine the $Fe^{3+}/\Sigma Fe$ ratio of perovskite under these relatively reducing conditions. Aluminous pyroxene starting materials were ground with an additional 20 wt% powdered metallic Fe and equilibrated in Fe capsules at 1,600 °C for run durations of up to five days. In most experiments 20 wt% ferropericlase was also added. Additional experiments in graphite capsules using a synthetic peridotite composition, without added metallic Fe, were performed at conditions slightly below and above the silicate solidus. The $Fe^{3+}/\Sigma Fe$ ratios of silicate perovskite in the recovered samples were measured using Mössbauer and electron energy loss spectroscopy[7] and are reported in Table 1. Figure 1a shows a typical run product. In addition to using a Fe capsule, distributing metallic Fe throughout the experimental charge is essential for ensuring redox equilibrium between the silicate and metal.

Figure 2 shows the Fe^{3+} versus the Al^{3+} content of perovskite in atoms per two-cation formula unit for samples equilibrated with metallic Fe at typical mantle temperatures. The shaded region encompasses results with uncertainties from similar experiments performed under more oxidizing conditions in the presence of Re and ReO_2 (refs 8, 9). The Fe^{3+} content of perovskite is coupled to the Al^{3+} concentration[8–10]. The nonlinear relationship between Al^{3+} and Fe^{3+} may result from a gradual change in the dominant trivalent cation incorporation mechanism—from one involving oxygen vacancies at low Al^{3+} concentrations, to a coupled substitution of trivalent cations at higher Al^{3+} concentrations[9]. Computer simulations indicate that such a coupled substitution remains favourable at least up to 100 GPa, that is, over most of the lower